Part I

Near-equilibrium critical dynamics

Introduction

Originally, the term *'dynamic critical phenomena'* was coined for time-dependent properties near second-order phase transitions in thermal *equilibrium*. The kinetics of phase transitions in magnets, at the gas–liquid transition, and at the normal- to superfluid phase transition in helium 4 were among the prominent examples investigated already in the 1960s. The *dynamic scaling hypothesis*, generalizing the scaling ansatz for the static correlation function and introducing an additional dynamic critical exponent, successfully described a variety of these experiments. Yet only the development of the systematic *renormalization group* (RG) approach for critical phenomena in the subsequent decade provided a solid conceptual foundation for phenomenological scaling theories. Supplemented with exact solutions for certain idealized model systems, and guided by invaluable input from computer simulations in addition to experimental data, the renormalization group now provides a general framework to explore not only the static and dynamic properties near a critical point, but also the large-scale and low-frequency response in stable thermodynamic phases. Scaling concepts and the renormalization group have also been successfully applied to phase transitions at zero temperature driven by quantum rather than thermal fluctuations. It is to be hoped that RG methods may help to classify the strikingly rich phenomena encountered in far-from-equilibrium systems as well. Recent advances in studies of simple reaction-diffusion systems, active to absorbing state phase transitions, driven lattice gases, and scaling properties of moving interfaces and growing surfaces, among others, appear promising in this respect.

The first part of this book focuses on equilibrium critical phenomena, dominated by strong *thermal fluctuations* near a thermodynamic instability. Here we introduce most of the fundamental concepts and analytical tools needed also for the analysis of quantum and non-equilibrium critical dynamics. We begin with a review of thermodynamic singularities and the behavior of the order parameter correlations near a critical point. In addition to simple mean-field theory as encompassed in the

generic Landau–Ginzburg approach, we briefly survey Wilson's momentum shell RG method. Next, we introduce the basic principles that will allow us to study inherently dynamic fluctuation phenomena. Chapter 2 covers linear response theory as well as a discussion of master, Fokker–Planck, and Langevin equations that capture stochastic kinetics on different description levels. We specifically highlight the restrictive detailed-balance conditions required to reach thermal equilibrium in the long-time limit. In the subsequent Chapter 3, we turn our attention to critical slowing down and the implications of the dynamic scaling hypothesis. The crucial influence of 'slow' diffusive conserved quantities besides the order parameter is elucidated.

Thereby equipped with a basic understanding of the relevant physical picture, we venture into more formal chapters on dynamic perturbation theory and the field-theoretic variant of the renormalization group procedure. These central chapters provide a powerful general analytic framework for many of the subsequent discussions. Chapter 4 contains a detailed exposition of the perturbation expansion for purely relaxational kinetics with either non-conserved or conserved order parameter. In Chapter 5, the renormalization program is explicitly carried through for these time-dependent Landau–Ginzburg models. The critical exponents are computed to lowest non-trivial loop order, where a small parameter for the perturbation series is given by the deviation $\epsilon = d_c - d$ from the (upper) critical dimension $d_c = 4$. We also explain how the emergence of massless Goldstone modes leads to generic scale invariance in the entire low-temperature phase of systems with broken continuous symmetry.

Chapter 6 explores the effect of additional conserved hydrodynamic modes and reversible non-linear mode couplings. Exploiting underlying symmetries, we derive scaling relations for the dynamic critical exponents associated with, e.g., the equilibrium critical dynamics of magnetic systems, superfluid helium 4, and binary liquids. A link is provided to self-consistent mode-coupling theory, a valuable tool for the calculation of scaling functions and quantitative comparison with experiments. Finally, Chapter 7 is concerned with phase transitions in quantum systems and quantum-critical phenomena. Here, we introduce coherent-state path integrals for bosonic and fermionic many-particle systems, and discuss several illustrative examples, most prominently the properties of boson superfluids and crossover features in quantum antiferromagnets.

1

Equilibrium critical phenomena

To set the stage for our subsequent thorough discussion of dynamic critical phenomena, we first review the theoretical description of second-order equilibrium phase transitions. (Readers already well acquainted with this material may readily move on to Chapter 2.) To this end, we compare the critical exponents following from the van-der-Waals equation of state for weakly interacting gases with the results from the Curie–Weiss mean-field approximation for the ferromagnetic Ising model. We then provide a unifying description in terms of Landau–Ginzburg theory, i.e., a long-wavelength expansion of the effective free energy with respect to the order parameter. The Gaussian model is analyzed, and a quantitative criterion is established that defines the circumstances when non-linear fluctuations need to be taken into account properly. Thereby we identify $d_c = 4$ as the upper critical dimension for generic continuous phase transitions in thermal equilibrium. The most characteristic feature of a critical point turns out to be the divergence of the correlation length that renders microscopic details oblivious. As a consequence, not only the correlation functions, but remarkably the thermodynamics as well of a critical system are governed by an emergent unusual symmetry: scale invariance. A simple scaling ansatz is capable of linking different critical exponents; as an application, we introduce the basic elements of finite-size scaling. Finally, a brief sketch of Wilson's momentum shell renormalization group method is presented, intended as a pedagogical preview of the fundamental RG ideas. Exploiting the scale invariance properties at the critical point, the scaling forms of the free energy and the order parameter correlation function are derived. The critical exponents are computed perturbatively to first order in $\epsilon = 4 - d$. Beginning with Chapter 4, we shall later venture into a more formal discussion of both static and dynamic critical phenomena, utilizing the framework of renormalized field theory based on non-linear Langevin stochastic equations of motion.

1.1 Mean-field theory

We begin our review with a brief discussion of the classic *mean-field theories* for the gas–liquid and para-/ferromagnetic equilibrium critical point.[1] The common feature of such mean-field approaches is that spatial fluctuations of the thermodynamic variable serving as the order parameter for the transition are neglected. Ordinarily, in a macroscopic system with $N \gg 1$ degrees of freedom, arguments akin to the central-limit theorem can be safely applied to any extensive thermodynamic quantity, whereupon one would expect its fluctuations relative to its mean ($\sim N$) to be of order $N^{-1/2}$. However, in the vicinity of a critical point, the thermodynamic response function associated with the order parameter diverges. This indicates that its mean-square thermal fluctuations become of order N^2 (in mean-field approximation) rather than N, and cannot generally be disregarded in the computation of thermodynamic potentials and correlation functions. Nevertheless, mean-field theories often provide qualitatively correct pictures of the essential physics and phase diagrams.

1.1.1 Van-der-Waals equation of state

The *van-der-Waals equation of state* for a weakly interacting gas,

$$P(T, V, N) = \frac{N k_{\mathrm{B}} T}{V - Nb} - \frac{N^2 a}{V^2} , \tag{1.1}$$

relates its pressure P to the volume V, temperature T, and particle number N. The parameter $b > 0$ stems from the short-range repulsions between the gas molecules, and corresponds to the average excluded volume per hard-core particle. This excluded volume repulsion naturally increases the gas pressure P. Attractive two-body molecular forces, on the other hand, will reduce the pressure by a term $\propto -(N/V)^2$. For weak long-range pair interactions, e.g., of the van-der-Waals form $V(r) \propto -1/r^6$ originating in fluctuating electric dipole moments, essentially only the radially averaged pair potential $\sim a$ matters, which leads to the second term in Eq. (1.1).

Typical van-der-Waals isotherms $P(v)$ at $T = \text{const.}$ are sketched in Fig. 1.1 as function of the reduced volume (inverse particle density) $v = V/N = 1/n$. At high temperatures $T \gg T_{\mathrm{c}}$, they approach the *universal* ideal gas law $PV = N k_{\mathrm{B}} T$, independent of the microscopic interaction parameters a and b. Upon lowering T, the isotherms develop an inflection point with decreasing slope. As we shall see, the critical temperature $T = T_{\mathrm{c}}$ is reached when this inflection point turns into

[1] More detailed descriptions can be found in most modern graduate level textbooks on equilibrium statistical mechanics, e.g.: Chaikin and Lubensky (1995), Pathria (1996), Cowan (2005), Schwabl (2006), Kardar (2007a, b), Reichl (2009), and Van Vliet (2010).

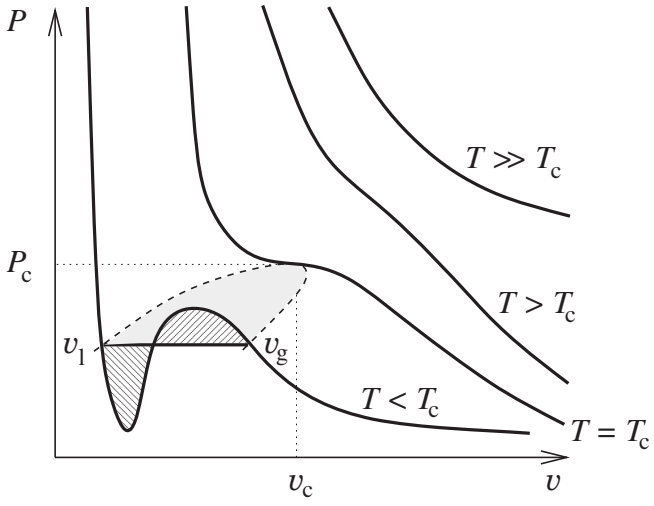

Fig. 1.1 Sketch of van-der-Waals isotherms in different temperature regimes. The critical point (v_c, P_c) (dotted) and the coexistence curve (dashed), which encloses the coexistence area (grey), are indicated. For $T < T_c$, Maxwell's construction demands that the shaded areas delimited by v_l and v_g be equal.

a saddle point with horizontal tangent. For $T < T_c$, the function $P(v)$ has two extrema. However, the van-der-Waals equation becomes unphysical in the region where $(\partial P/\partial v)_T > 0$, because thermodynamic stability requires the *isothermal compressibility* $\kappa_T = -v^{-1}(\partial v/\partial P)_T$ to be positive in thermal equilibrium. In fact, in the grand-canonical ensemble it is related to the mean-square particle number fluctuations,

$$\kappa_T = \frac{v(\Delta N)^2}{N k_B T} > 0 \,. \tag{1.2}$$

We interpret the instability for $T < T_c$ to indicate *phase separation* between a more dilute *gaseous* (g) state and a denser *liquid* (l) phase. In equilibrium, these two phases are not only at the same temperature and pressure, but must have identical chemical potentials $\mu_g = \mu_l$. Following Maxwell's construction, we thus replace the van-der-Waals isotherm for $v_l < v < v_g$ with a line of constant pressure $P_0(T)$. Employing the Gibbs–Duhem relation $\mu = G/N$ and the differential of the free enthalpy (Gibbs free energy) $dG = -SdT + VdP + \mu dN$, we have for $T, N = \text{const.}$:

$$0 = \mu_g - \mu_l = \int_{v_l}^{v_g} v \, \mathrm{d}P \,, \tag{1.3}$$

which represents the oriented area under the $v(P)$ curve. Therefore v_l and v_g are uniquely determined by the condition that the shaded areas in Fig. 1.1 be equal.

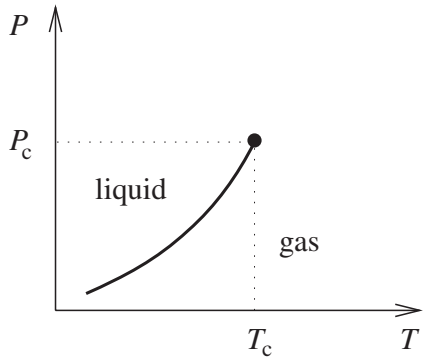

Fig. 1.2 Phase diagram in the (T, P) plane. The vapor pressure curve $P_0(T)$ separating the gas and liquid phases terminates at the critical point (T_c, P_c).

As the pressure is increased at constant temperature $T < T_c$, the density *discontinuously* jumps from $n_g = 1/v_g$ to $n_l = 1/v_l$; the associated change in entropy per particle s releases the *latent heat* $q_L = T(s_g - s_l)$. Thus, for $T < T_c$, the van-der-Waals equation describes a *first-order* gas–liquid phase transition.

The *phase coexistence region* (the surface bounded by the dashed line in Fig. 1.1) does not extend beyond T_c. Correspondingly, the *vapor pressure curve* $P_0(T)$, defined as the projection of the coexistence surface onto the (T, P) plane, terminates at the *critical point* (Fig. 1.2). While the vapor pressure curve marks a first-order transition line, at T_c the latent heat vanishes (see Problem 1.1), and the gas–liquid phase transition becomes of *second order*. This very special critical point in the phase diagram is defined by the conditions $(\partial P/\partial v)_{T_c, v_c} = 0 = (\partial^2 P/\partial v^2)_{T_c, v_c}$, and $P_c = P(T_c, v_c)$. Notice that the first equation implies the divergence of κ_T in the thermodynamic limit $N, V \to \infty$ (with n held fixed). Inserting the van-der-Waals equation of state, one readily identifies

$$v_c = 3b \,, \quad k_B T_c = \frac{8a}{27b} \,, \quad P_c = \frac{a}{27b^2} \,, \tag{1.4}$$

and hence $P_c v_c / k_B T_c = 3/8$ universally for *all* fluids. In fact, upon rescaling to quantities measured relative to their critical values, $\varphi = (v - v_c)/v_c$, $\tau = (T - T_c)/T_c$, and $p = (P - P_c)/P_c$, the microscopic parameters a and b disappear from the equation of state (1.1) entirely:

$$1 + p = \frac{4(1+\tau)}{1 + \frac{3}{2}\varphi} - \frac{3}{(1+\varphi)^2} \,. \tag{1.5}$$

According to this *law of corresponding states*, when expressed in terms of φ, τ, and p, the equations of states for *all* weakly interacting fluids should, at least approximately, be described by the same *universal* relation.

We may now derive the properties in the vicinity of the critical point by expanding Eq. (1.5) for small φ, retaining only the lowest-order non-vanishing terms. This yields

$$p \approx 4\tau - 6\tau\varphi - \frac{3}{2}\varphi^3 \,, \tag{1.6}$$

wherefrom we immediately infer the cubic *critical isotherm* ($\tau = 0$),

$$-p \approx \frac{3}{2}\varphi^3 \,. \tag{1.7}$$

For the *vapor pressure curve*, because of the antisymmetry near v_c, we may simply put $\varphi = 0$, and obtain $p_0 \approx 4\tau$ ($\tau < 0$). This sets the reference point for determining the spontaneous specific volume change at the phase transition. The *coexistence curve* is defined as the projection onto the (v, P) plane; hence $-6\tau\varphi = \frac{3}{2}\varphi^3$, or

$$\varphi_g = -\varphi_l \approx (-4\tau)^{1/2} \quad (\tau < 0) \tag{1.8}$$

on the gas and liquid side, respectively (compare the parabolic form of the dashed curve in Fig. 1.1). The specific volume difference $\varphi_g - \varphi_l = 2\varphi_g$, setting on *continuously* at $T = T_c$, may serve as the phase separation *order parameter*. We proceed to compute the isothermal compressibility,

$$\kappa_T \, P_c = -\left(\frac{\partial\varphi}{\partial p}\right)_\tau \approx \frac{1}{6\tau + \frac{9}{2}\varphi^2} \approx \begin{cases} 1/6\tau \,, & \tau > 0 \,, \\ 1/12|\tau| \,, & \tau < 0 \,. \end{cases} \tag{1.9}$$

Hence, $\kappa_T = \kappa_\pm |\tau|^{-1}$ diverges on both sides of the critical point, but with different amplitudes, $\kappa_+/\kappa_- = 2$. According to Eq. (1.2), this implies very large particle number or density fluctuations. These cause strong light scattering near the critical point, a phenomenon known as *critical opalescence* (see Section 1.1.3). Finally, employing the caloric equation of state, one finds that the specific heat C_v displays a discontinuity $\Delta C_v = \frac{9}{2} N k_B$ at T_c (Problem 1.1).

1.1.2 Mean-field theory for the ferromagnetic Ising model

In the theory of magnetism, and for the understanding of phase transitions and critical phenomena, the *(Lenz–)Ising model* has played a pivotal role. Its degrees of freedom are N discrete spin variables $\sigma_i = \pm 1$ on d-dimensional lattice sites x_i. Subject to an external magnetic field h (in units of energy), the energy of a given configuration of $\{\sigma_i\}$ is given by the Ising Hamiltonian

$$H(\{\sigma_i\}) = -\frac{1}{2}\sum_{i,j=1}^{N} J_{ij}\sigma_i\sigma_j - h\sum_{i=1}^{N}\sigma_i \,, \tag{1.10}$$

with *exchange couplings* J_{ij}. Notice that in the absence of h, this Hamiltonian is symmetric with respect to sign inversion $\sigma_i \to -\sigma_i \ \forall i$. Henceforth, we shall assume *ferromagnetic* interactions, favoring parallel spin alignment, and require translational invariance, $J_{ij} = J(x_i - x_j) \geq 0$. We may then perform a discrete Fourier transform[2]

$$J(q) = \sum_i J(x_i)\, \mathrm{e}^{-iq\cdot x_i} \ . \tag{1.11}$$

In equilibrium statistical mechanics, the task now is to evaluate the *canonical partition sum* over all possible spin configurations,

$$Z(T, h, N) = \sum_{\{\sigma_i = \pm 1\}} \mathrm{e}^{-H(\{\sigma_i\})/k_\mathrm{B}T} \ . \tag{1.12}$$

Thermodynamic properties are then given as averages of appropriate functions of the binary spin variables σ_i,

$$\langle A(\{\sigma_i\})\rangle = \frac{1}{Z} \sum_{\{\sigma_i = \pm 1\}} A(\{\sigma_i\})\, \mathrm{e}^{-H(\{\sigma_i\})/k_\mathrm{B}T} \ , \tag{1.13}$$

and may often be obtained via appropriate partial derivatives with respect to temperature T or field h. In one dimension, this program can be easily carried through explicitly, see Problem 1.2. Even in two dimensions, the Ising model may be solved exactly, albeit with considerably greater effort. In higher dimensions, it has, however, eluded any such attempts, and one must resort to approximations.

In Curie–Weiss mean-field theory, essentially the effective 'local' field

$$h_{\mathrm{eff},i} = -\frac{\partial H}{\partial \sigma_i} = h + \sum_j J_{ij}\sigma_j \tag{1.14}$$

is replaced with its average $\langle h_\mathrm{eff}\rangle = h + \widetilde{J}m$, where $\widetilde{J} = J(q=0) = \sum_i J(x_i)$, and $m = \langle \sigma_i \rangle = M/N$ denotes the magnetization per spin. We would clearly expect this approximation to work best when the exchange interactions are long-range, and their effect on any site roughly uniform; or in high dimensions, when the interactions with many neighboring sites average out local fluctuations. The Ising Hamiltonian thus becomes that of a simple two-state paramagnet, subject to the combined external and internal field $\langle h_\mathrm{eff}\rangle$. The magnetization m can then be determined self-consistently. More precisely, we decompose the local spin into its average and fluctuation, $\sigma_i = m + (\sigma_i - \langle\sigma_i\rangle)$, whence $\sigma_i\,\sigma_j = m^2 + m(\sigma_i - \langle\sigma_i\rangle + \sigma_j - \langle\sigma_j\rangle) + (\sigma_i - \langle\sigma_i\rangle)(\sigma_j - \langle\sigma_j\rangle)$. Upon

[2] Throughout this book, vector quantities will not be specifically indicated through arrows or boldface typing. Neither will distinct symbols be used for the Fourier transforms of scalar or vector fields; if required to avoid confusion, rather the arguments will be noted explicity.